

## **General Disclaimer**

### **One or more of the Following Statements may affect this Document**

- This document has been reproduced from the best copy furnished by the organizational source. It is being released in the interest of making available as much information as possible.
- This document may contain data, which exceeds the sheet parameters. It was furnished in this condition by the organizational source and is the best copy available.
- This document may contain tone-on-tone or color graphs, charts and/or pictures, which have been reproduced in black and white.
- This document is paginated as submitted by the original source.
- Portions of this document are not fully legible due to the historical nature of some of the material. However, it is the best reproduction available from the original submission.

# Effect of the Amount of $\text{Na}_2\text{SO}_4$ on the High Temperature Corrosion of Udimet-700

(NASA-TM-83459) EFFECT OF THE AMOUNT OF  
 $\text{Na}_2\text{SO}_4$  ON THE HIGH TEMPERATURE CORROSION OF  
UDIMET-700 (NASA) 19 p HC A02/MF A01

N83-34016

CSSL 11F

G3/26

Unclas  
36117

A. K. Misra and F. J. Kohl  
*Lewis Research Center*  
*Cleveland, Ohio*



Prepared for the  
Annual Meeting of the Electrochemical Society  
San Francisco, California, May 8-13, 1983

**NASA**

# EFFECT OF THE AMOUNT OF $\text{Na}_2\text{SO}_4$ ON THE HIGH TEMPERATURE CORROSION OF UDIMET-700

A. K. Misra\* and F. J. Kohl

National Aeronautics and Space Administration  
Lewis Research Center  
Cleveland, Ohio 44135

## ABSTRACT

E-1774

The corrosion of Udimet-700, coated with different doses of  $\text{Na}_2\text{SO}_4$ , was studied in an isothermal thermogravimetric test in the temperature range 900 to 950° C. The weight gain curve can be characterized by five distinct stages: (1) an initial period of linear corrosion; (2) an induction period; (3) a period of accelerated corrosion; (4) a period of decelerating corrosion; and, (5) a period of parabolic oxidation. The time required for the failure of the alloy increases with an increase in the amount of  $\text{Na}_2\text{SO}_4$ , reaches a peak and then decreases with further increase in the amount of  $\text{Na}_2\text{SO}_4$ . For low and intermediate doses (0.3 to 2.0 mg/cm<sup>2</sup>), the catastrophic failure of the material occurs by the formation of  $\text{Na}_2\text{MoO}_4$  and interaction of the liquid  $\text{Na}_2\text{MoO}_4$  with the alloy. For heavy doses, the degradation of the material is due to the formation of large amounts of sulfides.

## INTRODUCTION

Hot corrosion in combustion turbine engines is associated with the deposition of  $\text{Na}_2\text{SO}_4$  on turbine blade and vane surfaces. In the past, many investigators (1, 2, 3, 4) have studied the mechanism of hot corrosion of superalloys. A layer of molten  $\text{Na}_2\text{SO}_4$  on the alloy surface can cause degradation of the alloy by two different but interrelated mechanisms: (1) a fluxing process, in which the molten  $\text{Na}_2\text{SO}_4$  dissolves the protective oxides formed on the alloy; and (2) a sulfidation process, in which the molten  $\text{Na}_2\text{SO}_4$  introduces sulfur into the alloy. These mechanisms are based largely on observations made from laboratory experiments, wherein given amounts of  $\text{Na}_2\text{SO}_4$  are sprayed on to samples which are oxidized in a low velocity gas flow. However, laboratory tests do not necessarily simulate actual turbine operating conditions. The procedures which more closely simulates the actual service conditions are the high velocity burner rig tests. Also, there is no definite correlation between the results from laboratory salt-spray tests and those from burner rig experiments. Laboratory salt-spray tests usually show distinct features of a fluxing type of attack (1, 2, 3), where as the burner rig experiments usually show a sulfidation type

\*NRC-NASA Resident Research Associate.

of attack (5). These differences in corrosion behavior are primarily due to two factors: (1) high gas flow velocity in the burner rigs, and (2) a continuous deposition of  $\text{Na}_2\text{SO}_4$  onto the sample. When the deposition of  $\text{Na}_2\text{SO}_4$  is continuous, the relationship between the rate of deposition and the rate of corrosion should be known in order to predict the useful lifetime of the turbine blading materials.

The work reported here was undertaken to study the corrosion of a nickel-base superalloy, U-700, as a function of the amount of  $\text{Na}_2\text{SO}_4$  on the alloy. The alloy U-700 was chosen because of its high molybdenum content (5 wt percent) and previous burner rig testing with this alloy. A survey of the corrosion literature shows that the differences between the laboratory tests and burner rig experiments are most significant for alloys containing molybdenum (6). The results presented here are considered as a first step to understanding the link between rate of deposition and rate of corrosion for the alloy U-700.

## EXPERIMENTAL PROCEDURE

The composition of wrought U-700 is given in weight percent as Co, 17.5; Cr, 14.8; Mo, 5.03; Al, 4.40; Ti, 2.95; Fe, 0.19; C, 0.06; B, 0.04; Mn, 0.01; Ni Balance. Test samples were coupons measuring 2.30 x 1.05 x 0.23 cm with a hangdown hole at one end. All sample surfaces were glass-bead blasted to given a uniform matte finish. The  $\text{Na}_2\text{SO}_4$  was applied by air brushing a saturated  $\text{Na}_2\text{SO}_4$  solution onto coupons, heated on a hot plate to 200° C. Visual examination showed the  $\text{Na}_2\text{SO}_4$  deposit to be uniform over the sample. The  $\text{Na}_2\text{SO}_4$ -coated coupons were oxidized in flowing  $\text{O}_2$ , the flow rate being of the order of 2.03 cm/sec, in an isothermal thermogravimetric test in the temperature range 900 to 950° C. Weight gain measurements were made with a Cahn R-100 microbalance. The samples, corroded for different lengths of time, were washed in hot distilled water, and the solution was analysed for various water-soluble elements.

## RESULTS AND DISCUSSION

### Kinetics

The kinetics of corrosion of U-700, coated with different doses of  $\text{Na}_2\text{SO}_4$  in the range of 0 to 6.5 mg/cm<sup>2</sup> and oxidized at 950° C in 1 atm.  $\text{O}_2$ , are shown in Fig. 1 and 2. For doses greater than 0.3 mg/cm<sup>2</sup>, the corrosion is catastrophic and the weight gain versus time curve can be characterized by five distinct stages: (1) an initial period of linear weight gain; (2) an induction period; (3) a period of acceleration corrosion, (4) a period decelerating corrosion; and, (5) a period of parabolic oxidation, during which the weight gain versus time curve is almost identical to that oxidation in  $\text{O}_2$ . The total weight gain during the initial period of linear corrosion increases with an increased in the amount of  $\text{Na}_2\text{SO}_4$  on the sample. For a small dose of 0.3 mg/cm<sup>2</sup>, the total weight gain during this period is about 1.2 mg/cm<sup>2</sup>, whereas for heavy doses, e.g., 6.5 mg/cm<sup>2</sup>, the total weight gain during this period is of the order 15 mg/cm<sup>2</sup>. For the heavy doses the weight gain during this initial period is sufficient to destroy the structural integrity of the alloy. The length of the induction period increases with an increase in the amount of  $\text{Na}_2\text{SO}_4$  up to a dose of

about  $1.8 \text{ mg/cm}^2$ , then the induction period length decreases with further increase in the amount of  $\text{Na}_2\text{SO}_4$ . For very small doses, e.g.,  $0.3 \text{ mg/cm}^2$ , the induction period is of the order of 2 to 3 hr. and cannot be clearly distinguished in the weight gain versus time curve. The total weight gain during the induction period increases with an increase in the amount of  $\text{Na}_2\text{SO}_4$  on the sample. The total weight gain at the end of the period of decelerating corrosion is observed to increase with an increase in the amount of  $\text{Na}_2\text{SO}_4$ . For the heavier doses, the period of decelerating corrosion and the period of parabolic oxidation are not shown in Fig. 1 and 2 in order to maintain clarity in presenting other details of the curves.

Fig. 3 shows the thermogravimetric test results at  $900^\circ \text{C}$ . The general features of the weight gain versus time curve are the same as those at  $950^\circ \text{C}$ . However, the length of the induction period for low and intermediate doses increases considerably at this temperature. For example, for a dose of  $1.47 \text{ mg/cm}^2$  of  $\text{Na}_2\text{SO}_4$ , the induction period is of the order of 300 hr.

### Analysis of the Water Soluble Elements

The amounts of various water-soluble elements recovered from samples oxidized for different lengths of time are shown in Fig 4 for two different doses of  $\text{Na}_2\text{SO}_4$  ( $0.3$  and  $3.13 \text{ mg/cm}^2$ ). The Cr, Mo, and  $\text{SO}_4$  concentrations in the solution are due to the presence of  $\text{Na}_2\text{CrO}_4$ ,  $\text{Na}_2\text{MoO}_4$ , and  $\text{Na}_2\text{SO}_4$  respectively. It can be seen that for both low and high doses, most of the  $\text{Na}_2\text{SO}_4$  is converted to  $\text{Na}_2\text{CrO}_4$  during the first hour of corrosion. A comparison of the thermogravimetric curves with the results of the chemical analyses shows that the end of induction period is marked by the conversion of  $\text{Na}_2\text{CrO}_4$  to  $\text{Na}_2\text{MoO}_4$ . In the first hour of corrosion, the analysis of the soluble elements shows the presence of small amounts of molybdenum, however, large quantities of  $\text{Na}_2\text{MoO}_4$  are formed only at the end of the induction period.

### Scale Morphology

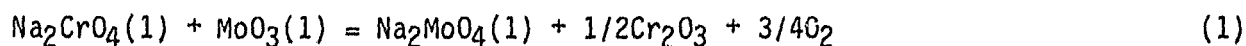
Initial period of linear weight gain. - When the  $\text{Na}_2\text{SO}_4$ -coated alloy is oxidized, during the transient stage of oxidation (for first few minutes only), the surface Mo carbides plus Ti and Cr oxidize to form  $\text{MoO}_3$ ,  $\text{TiO}_2$  and  $\text{Cr}_2\text{O}_3$  respectively. The  $\text{Cr}_2\text{O}_3$  and  $\text{MoO}_3$  dissolve in  $\text{Na}_2\text{SO}_4$  to form  $\text{Na}_2\text{CrO}_4$  and  $\text{Na}_2\text{MoO}_4$  respectively, and this accounts for the small amount of water soluble molybdenum that was observed during the first hour of corrosion. For a time period beyond this transient stage of oxidation, the scale consists of an external layer of  $\text{Cr}_2\text{O}_3 + \text{TiO}_2$  and internal Cr,Ti sulfides. The scale morphologies during the first 3 hr of corrosion are compared in Fig. 5. Because for a very low dose of  $\text{Na}_2\text{SO}_4$ , e.g  $0.3 \text{ mg/cm}^2$ , the initial period of linear weight gain lasts only for an hour or so, the scale morphology after 25 minutes of corrosion is shown in Fig. 5 for the low dose. It can be seen that the extent of internal sulfidation and the morphology of the internal sulfides are strongly dependent on the amount of  $\text{Na}_2\text{SO}_4$ . The extent of internal sulfidation during the first 3 hr. increases with an increase in the amount of  $\text{Na}_2\text{SO}_4$ . For low doses, the Cr,Ti sulfides are formed as random, discrete particles, whereas for heavy doses, the sulfides are preferentially formed along the grain boundaries. The depth of grain boundary sulfide penetration increases with an increase in the amount of  $\text{Na}_2\text{SO}_4$ . For heavy doses, in addition to the grain boundary sulfides, some random and discrete internal sulfide particles are also observed; however, the bulk of the sulfides are formed

along the grain boundaries. The thickness of the external oxide scale also increases with an increase in the amount of  $\text{Na}_2\text{SO}_4$ . However, for heavier doses, the external scale contains many unoxidized grains, which are depleted in Cr, Ti, but rich in Ni, Co and Mo. It appears that when the alloy is oxidized beneath a thick layer of  $\text{Na}_2\text{SO}_4$ , Cr, Ti oxides and/or sulfides are preferentially formed along the grain boundaries and this leaves the grains depleted in Cr and Ti.

For the heavier doses, the initial period of linear corrosion continues much longer than 3 hr. and therefore, it is instructive to examine the scale morphologies just at the end of this period. The scale morphologies for two different doses of  $\text{Na}_2\text{SO}_4$  (3.13 and 4.36  $\text{mg}/\text{cm}^2$ ) are shown in Fig. 6 and 7 respectively. For both doses, the grain boundary sulfides have oxidized resulting in a porous  $\text{Cr}_2\text{O}_3 + \text{TiO}_2$  scale. The grains, which are rich in Ni, Co, Mo are also partially oxidized. For the 3.13  $\text{mg}/\text{cm}^2$  sample, only a few random discrete internal sulfide particles can be observed to be present at the scale-metal interface. For the 4.36  $\text{mg}/\text{cm}^2$  sample, some grain boundary sulfides are observed to be present at the scale-metal interface. The amount of sulfides, retained at the end of the initial period of linear corrosion, increases with an increase in the amount of  $\text{Na}_2\text{SO}_4$ . These results clearly show that all of the sulfur, released by the oxidation of sulfides, does not enter the alloy again as has been proposed by Spengler and Viswanathan (7). The extent to which the sulfur, released by the oxidation of sulfides, enters the alloy and produces more sulfides is dependent on the extent of grain boundary sulfide penetration. The greater the depth of grain boundary sulfide penetration, the larger will be the amount of sulfides retained in the alloy after the oxidation of the sulfides. This is related to the ease with which the sulfurous gases, generated by the oxidation of sulfides, can escape to the atmosphere. If the sulfurous gases are generated deep in the alloy, they have to travel a long tortuous path to reach the atmosphere. Therefore, the sulfurous gases, generated by the oxidation of sulfides deep in the alloy, will reenter the alloy and form more sulfides. The present results also suggest that the bulk of the sulfides are formed within 2 to 3 hrs from the start of corrosion, and the rapid weight gain in the initial period of linear corrosion is due to (1) oxidation of grain boundary Cr, Ti sulfides; and (2) oxidation of the grains, which are depleted in Cr, Ti but rich in Ni, Co, and Mo. For the heavy doses (3.5 to 6.5  $\text{mg}/\text{cm}^2$ ), the extent of corrosion at the end of the initial period of linear corrosion is sufficient to destroy the structural integrity of the alloy.

Induction period. - During the induction period, the scale growth takes place by diffusion of Cr, Ti from the depleted region. Also, for the heavier doses of  $\text{Na}_2\text{SO}_4$  some of the grain boundary sulfides are still present. These sulfides oxidize during the induction period, thus contributing to the weight gain. It was mentioned earlier that the amount of sulfides, retained at the end of the initial period of linear corrosion, increases with an increase in the amount of  $\text{Na}_2\text{SO}_4$ . Therefore, the rate of weight gain during the induction period increases with an increase in the amount of  $\text{Na}_2\text{SO}_4$ . At the end of the initial period of linear corrosion, the scale is also covered with a layer of liquid  $\text{Na}_2\text{CrO}_4$ . During the induction period, the  $\text{Na}_2\text{CrO}_4$  melt penetrates through the external scale, which is shown in Fig. 8. The external scale is composed of a porous layer, through which the melt had penetrated and a denser oxide layer.

From the chemical analysis, it is known that the end of induction period is marked by the formation of  $\text{Na}_2\text{MoO}_4$ . The formation of  $\text{Na}_2\text{MoO}_4$  is accompanied by a sharp decrease in the  $\text{Na}_2\text{CrO}_4$  concentration, which suggests that  $\text{Na}_2\text{MoO}_4$  is formed by reaction of  $\text{Na}_2\text{CrO}_4$  with the Mo compounds. Fig. 8 shows the  $\text{Na}_2\text{CrO}_4$  melt penetrating the external  $\text{Cr}_2\text{O}_3 + \text{TiO}_2$  scale and thus after sufficient length of time, the melt reaches the scale-metal interface. At the scale-metal interface,  $\text{Na}_2\text{CrO}_4(1)$  comes in contact with the region, depleted in Cr and Ti but rich in Ni, Co and Mo. The  $\text{Na}_2\text{MoO}_4$  can be formed by two different mechanisms: (1) During the induction period, the external scale loses contact with the underlying alloy because of growth stresses, vacancy injection etc, and the oxidation of the depletion region, which is rich in Ni, Co and Mo, takes place. From thermodynamic considerations, the oxidation of Ni-Co-Mo alloy should produce a  $\text{MoO}_3$  scale because of the greater stability of  $\text{MoO}_3$  compared to that of  $\text{NiO}$  or  $\text{CoO}$ . Then  $\text{Na}_2\text{CrO}_4(1)$  reacts with  $\text{MoO}_3$  to form  $\text{Na}_2\text{MoO}_4$  by the reaction:



$$\Delta G^\circ_{1200\text{K}} = -15.594 \text{ Kcal}$$

(2) The  $\text{Na}_2\text{MoO}_4(1)$  is formed by the direct interaction of the  $\text{Na}_2\text{CrO}_4(1)$  with Mo in the depletion region. While direct reaction of  $\text{Na}_2\text{CrO}_4(1)$  with Ni or Co is not thermodynamically favorable,  $\text{Na}_2\text{CrO}_4(1)$  can react with Mo to form  $\text{Na}_2\text{MoO}_4(1)$  by the reaction:



$$\Delta G^\circ_{1200\text{K}} = -26.713 \text{ Kcal}$$

Because both mechanisms of  $\text{Na}_2\text{MoO}_4$  formation depend on  $\text{Na}_2\text{CrO}_4(1)$  and the depletion region, the length of the induction period is dependent on the time required for the  $\text{Na}_2\text{CrO}_4(1)$  to reach the depletion region. It was seen earlier that  $\text{Na}_2\text{CrO}_4(1)$  penetrates the external  $\text{Cr}_2\text{O}_3 + \text{TiO}_2$  scale, thus, the time required for the  $\text{Na}_2\text{CrO}_4(1)$  to penetrate the oxide scale and reach the scale-metal interface depends on the thickness and porosity of the external scale. Both of these factors, e.g, thickness and porosity of the external scale are controlled by the events during the initial period of linear corrosion.

The scale morphologies shown in Fig. 5 indicate that, for low to intermediate doses of  $\text{Na}_2\text{SO}_4$ , the thickness of the external scale at the end of the initial period of linear corrosion increases with an increase in the amount of  $\text{Na}_2\text{SO}_4$ . Therefore, the time required for  $\text{Na}_2\text{CrO}_4(1)$  to penetrate the oxide scale and reach the scale-metal interface increases with an increase in the amount of  $\text{Na}_2\text{SO}_4$ . This results in an increase in the length of the induction period with an increase in the amount of  $\text{Na}_2\text{SO}_4$ .

For heavier doses, the scale consists of many unoxidized grains, which are rich in Ni, Co, and Mo. This is due to the preferential formation of Cr, Ti oxides/sulfides along the grain boundaries. Also the external scale, produced by the oxidation of grain boundary sulfides is porous. Therefore, the time required for the  $\text{Na}_2\text{CrO}_4(1)$  to reach the region, rich in Ni, Co, and Mo, is less. These factors contribute to the decrease in the length of the induction

period as the scale morphology changes from a thick  $\text{Cr}_2\text{O}_3 + \text{TiO}_2$  scale with discrete internal sulfides to an external scale containing grain boundary Cr, Ti oxides/sulfides and unoxidized Ni-Mo-Co-rich grain. The extent of grain boundary oxidation/sulfidation increases with an increase in the amount of  $\text{Na}_2\text{SO}_4$ , thus, decreasing the length of the induction period with an increase in the amount of  $\text{Na}_2\text{SO}_4$ .

Period of acceleration corrosion, decelerating corrosion, and of parabolic oxidation. - The period of accelerated corrosion is marked by the formation of  $\text{Na}_2\text{MoO}_4$ (1). The typical scale morphology for a corroded sample is shown in Fig. 9. The scale morphology shows a highly porous and striated external scale. There is severe grain boundary penetrations by liquid  $\text{Na}_2\text{MoO}_4$  at the scale-metal interface. The  $\text{Na}_2\text{MoO}_4$ , because of its low melting points (m.p. =  $689^\circ\text{C}$ ), is very fluid and easily penetrates along the alloy grain boundaries. This penetrating action lifts the metal grains from the alloy and this destroys the structural integrity of the alloy. When the alloy grains are lifted and oxidized, they form oxides like NiO,  $\text{Cr}_2\text{O}_3$ , CoO,  $\text{Al}_2\text{O}_3$  etc. The reaction of  $\text{Na}_2\text{MoO}_4$  with the oxides can form compounds such as  $\text{Cr}_2\text{O}_3 \cdot \text{MoO}_3$ ,  $\text{Al}_2\text{O}_3 \cdot \text{MoO}_3$ ,  $\text{NiO} \cdot \text{MoO}_3$  etc. EDAX analysis of the porous oxides indeed shows the presence of the metallic elements in these compounds (Fig. 9). The phase diagrams for the binary  $\text{Na}_2\text{MoO}_4$ -NiO $\cdot$ MoO $_3$  and  $\text{Na}_2\text{MoO}_4$  -  $\text{Al}_2\text{O}_3 \cdot \text{MoO}_3$  are not available. The  $\text{Na}_2\text{MoO}_4$  -  $\text{Cr}_2\text{O}_3 \cdot \text{MoO}_3$  phase diagram shows the presence of an eutectic (8). Assuming the phase diagram to be similar for the other binaries, the addition of  $\text{Cr}_2\text{O}_3 \cdot \text{MoO}_3$ , NiO $\cdot$ MoO $_3$  and  $\text{Al}_2\text{O}_3 \cdot \text{MoO}_3$  to  $\text{Na}_2\text{MoO}_4$  would be expected to reduce the melting point of the mixture up to the eutectic point. This makes the melt more fluid thus increasing its penetrating power and therefore increasing the rate of corrosion. When the eutectic point is reached, further addition of  $\text{Cr}_2\text{O}_3 \cdot \text{MoO}_3$ , NiO $\cdot$ MoO $_3$  or  $\text{Al}_2\text{O}_3 \cdot \text{MoO}_3$  increases the melting point of the mixture, thus decreasing the fluidity of the melt. This corresponds to the beginning of the period of decelerating corrosion. The melt penetration along the grain boundaries comes to a halt when the melt is saturated with  $\text{Cr}_2\text{O}_3 \cdot \text{MoO}_3$ , NiO $\cdot$ MoO $_3$  or  $\text{Al}_2\text{O}_3 \cdot \text{MoO}_3$  and a solid compound is formed. Clearly the extent of corrosion at the end of the period of decelerating corrosion is dependent on the amount of  $\text{Na}_2\text{MoO}_4$  formed, which in turn is dependent on the amount of  $\text{Na}_2\text{SO}_4$  applied. The greater the amount of  $\text{Na}_2\text{MoO}_4$  formed, the larger will be the amount of  $\text{Cr}_2\text{O}_3$ ,  $\text{Al}_2\text{O}_3$ , NiO that it can dissolve. Thus the extent of corrosion or metal recession increases with an increase in the amount of  $\text{Na}_2\text{MoO}_4$  formed.

Parallel experiments were conducted in which the U-700 samples were coated with different doses of  $\text{Na}_2\text{MoO}_4$  and oxidized in 1 atm.  $\text{O}_2$ . Fig. 10 gives the thermogravimetric results, which show that the extent of corrosion increases with an increase in the amount of  $\text{Na}_2\text{MoO}_4$ . As the amount of  $\text{Na}_2\text{MoO}_4$  formed increases with an increase in the amount of  $\text{Na}_2\text{SO}_4$  applied, the extent of corrosion at the end of the period of decelerating corrosion increases with an increase in the amount of  $\text{Na}_2\text{SO}_4$  on the sample.

After the formation of a solid compound, the alloy oxidizes in a manner similar to that of simple oxidation in  $\text{O}_2$ . The typical scale morphology at the end of the period of decelerating corrosion is shown in Fig. 11. A thick external porous layer had spalled off from the surface upon cooling. The presence of a thin solid Mo compound can be seen on the top of the external scale. The scale morphology consists of an external  $\text{Cr}_2\text{O}_3 + \text{TiO}_2$  scale and internal  $\text{Al}_2\text{O}_3$  tenacles. This is the typical scale morphology that is produced in pure oxidation.

## SUMMARY AND CONCLUSIONS

The present studies have shown that in laboratory furnace tests the corrosion of U-700 is strongly dependent on the amount of  $\text{Na}_2\text{SO}_4$  applied. The time required for the failure of the material increases with an increase in the amount of  $\text{Na}_2\text{SO}_4$ , reaches a peak, and then decreases again with further increase in the amount of  $\text{Na}_2\text{SO}_4$ . For small and intermediate doses, the degradation of the material takes place by the formation of  $\text{Na}_2\text{MoO}_4(1)$  and grain boundary penetration plus fluxing by the  $\text{Na}_2\text{MoO}_4$  melt. The time for material failure is related to the length of time required for the formation of  $\text{Na}_2\text{MoO}_4$ . Under these conditions, the molybdenum content of the alloy assumes a significant role in the overall corrosion process. For heavier doses, the material has undergone considerable degradation by the formation of grain boundary Cr,Ti-sulfides before  $\text{Na}_2\text{MoO}_4$  formation. Therefore, for the heavier doses, the Mo content of the alloy is not as important in the hot corrosion degradation process. A comparison of the results from the present investigation with those from burner rig tests(5) shows that the scale morphologies for the burner rig experiment samples correspond to those obtained in the laboratory with the heavy doses of  $\text{Na}_2\text{SO}_4$ . It appears, that the total amount of  $\text{Na}_2\text{SO}_4$  deposited on the sample is higher in the burner rigs because of a continuous deposition process. Also, in the burner rigs, the flow velocity is very high. Therefore,  $\text{Na}_2\text{CrO}_4$  is vaporized from the surface of the sample at a higher rate. In the absence of  $\text{Na}_2\text{CrO}_4$ ,  $\text{Na}_2\text{MoO}_4$  is not formed, thus, preventing a fluxing type of attack. Currently, work is in progress in understanding the corrosion of U-700 in burner rig experiments which will further elucidate the differences between the laboratory tests and the burner rig experiments.

## REFERENCES

1. J. A. Goebel, F. S. Pettit, and G. W. Goward, Metall. Trans., 4, 261 (1973)
2. N. S. Bornstein and M. A. DeCrescente, Metall. Trans., 2, 2875 (1971).
3. G. C. Fryburg, F. J. Kohl, C. A. Stearns, and W. L. Fielder, J. Electrochem. Soc., 129, 571 (1982).
4. D. M. Johnson, D. P. Whittle, and J. Stringer, Corros. Sci., 15, 649 (1975).
5. C. E. Lowell and D. L. Deadmore, Paper No. 121 presented at the 162nd meeting of the Electrochemical Society, Detroit, Michigan, Oct. 17-21, 1982.
6. K. R. Peters, D. P. Whittle, and J. Stringer, Corros. Sci., 16, 791 (1976).
7. C. J. Spengler and R. Viswanathan, Metall. Trans., 3, 161 (1972).
8. R. S. Roth, T. Negas, and L. P. Cook, "Phase Diagrams for Ceramists," Vol. 4, p 183, American Ceramic Society, Columbus, Ohio (1981).

ORIGINAL PAGE IS  
OF POOR QUALITY

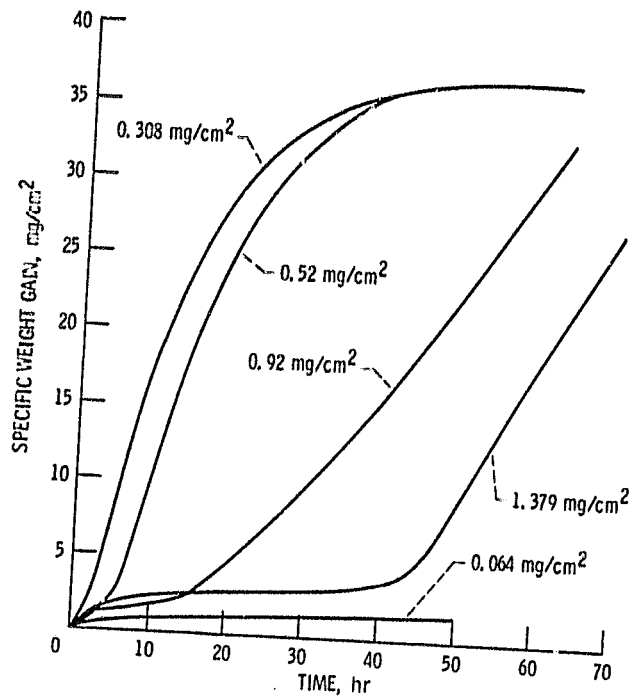


Figure 1. - Kinetics of hot corrosion of U-700 coated with different doses of  $\text{Na}_2\text{SO}_4$  and oxidized in 1 atm.  $\text{O}_2$  at  $950^\circ \text{C}$ .

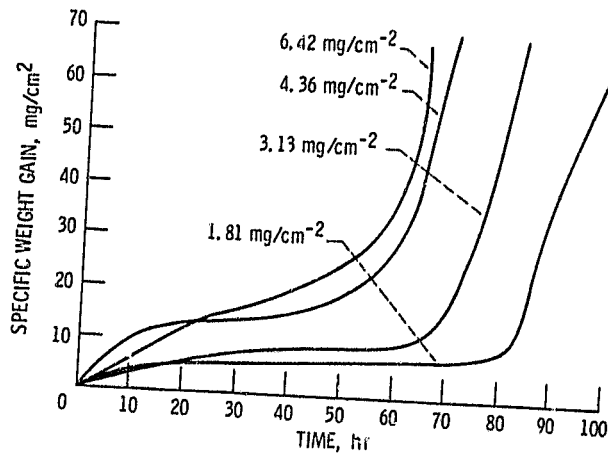


Figure 2. - Kinetics of hot corrosion of U-700 coated with different doses of  $\text{Na}_2\text{SO}_4$  and oxidized in 1 atm.  $\text{O}_2$  at  $950^\circ \text{C}$ .

# COMPARISON OF OF POOR QUALITY

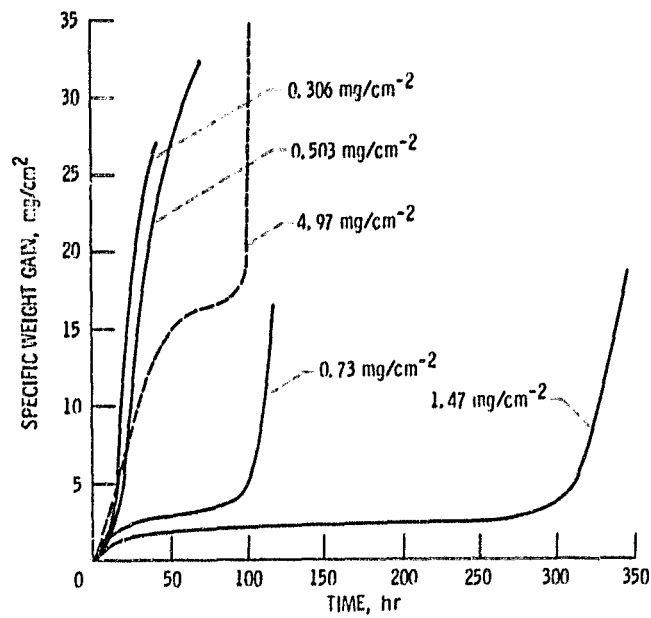


Figure 3. - Kinetics of hot corrosion of U-700 coated with different doses of  $\text{Na}_2\text{SO}_4$  and oxidized in 1 atm.  $\text{O}_2$  at  $900^\circ\text{C}$ .

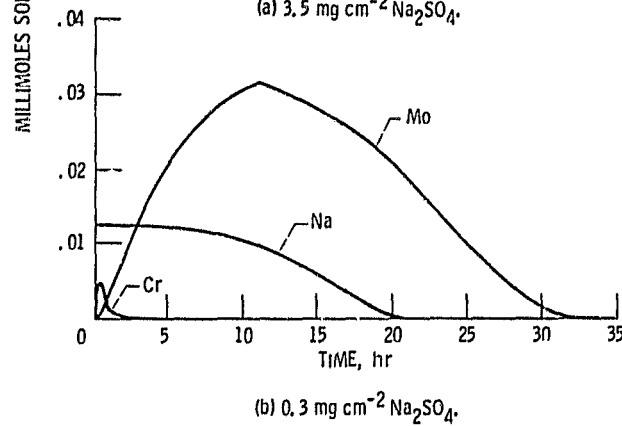
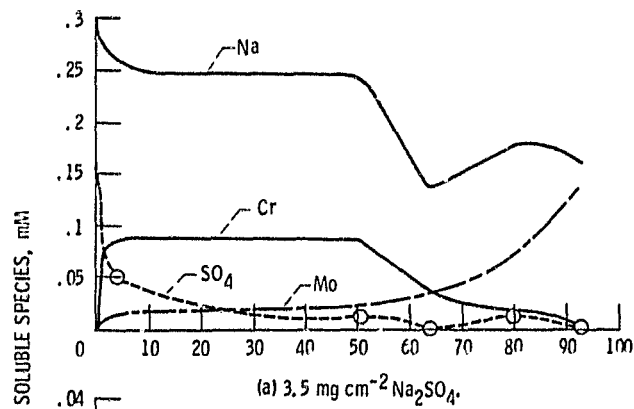


Figure 4. - Quantity of water soluble found after various times of hot corrosion testing at  $950^\circ\text{C}$ .

ORIGINAL PAGE IS  
OF POOR QUALITY

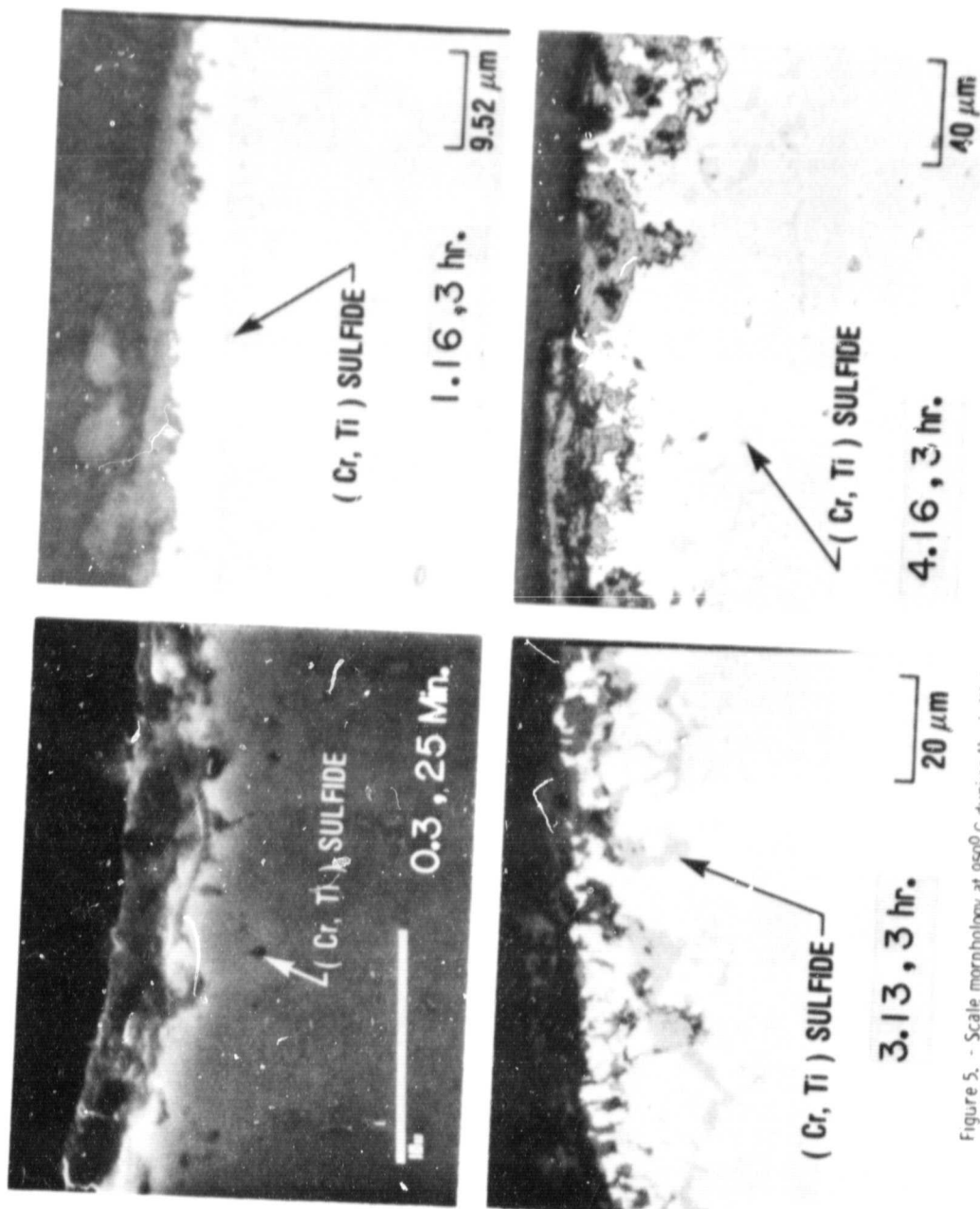


Figure 5. - Scale morphology at 950°C during the initial period of linear corrosion as a function of the amount of  $\text{Na}_2\text{SO}_4$ .

ORIGINAL PAGE IS  
OF POOR QUALITY

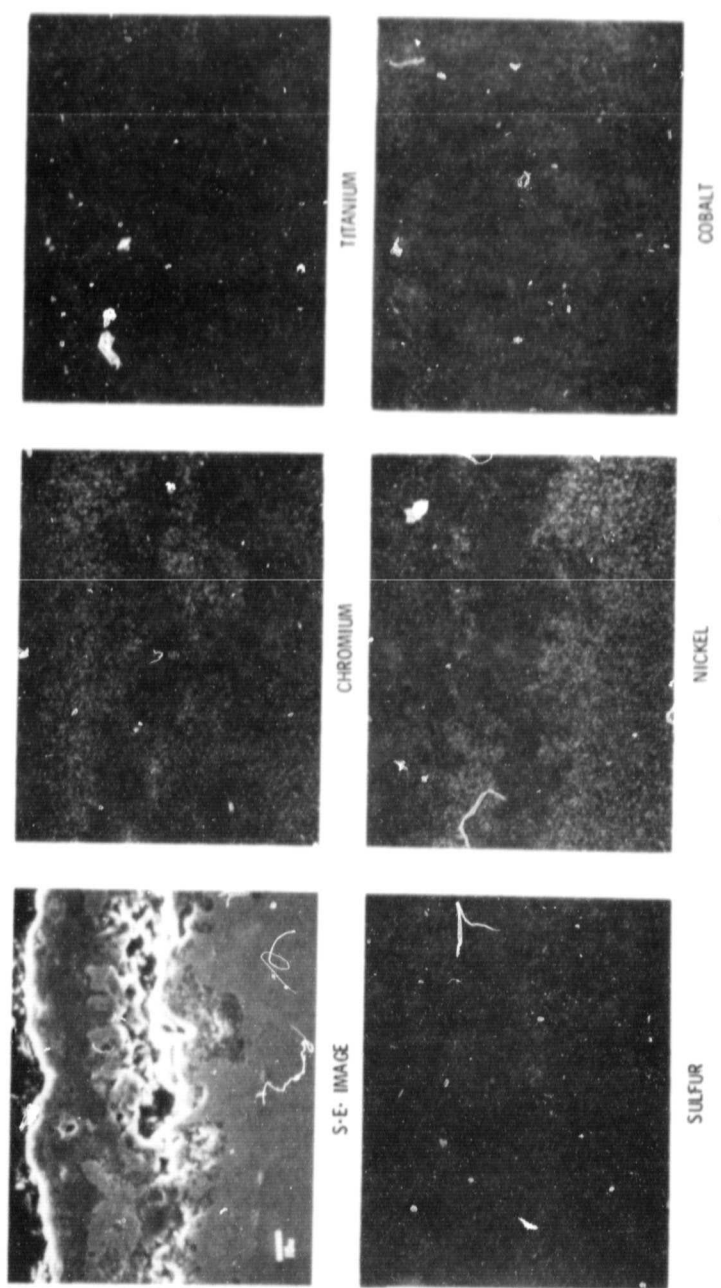


Figure 6. - S. E. image and X-ray maps for U-700 coated with 3.13 mg/cm<sup>2</sup> Na<sub>2</sub>SO<sub>4</sub> and oxidized at 950°C for 15 hours.

ORIGINAL PAGE IS  
OF POOR QUALITY

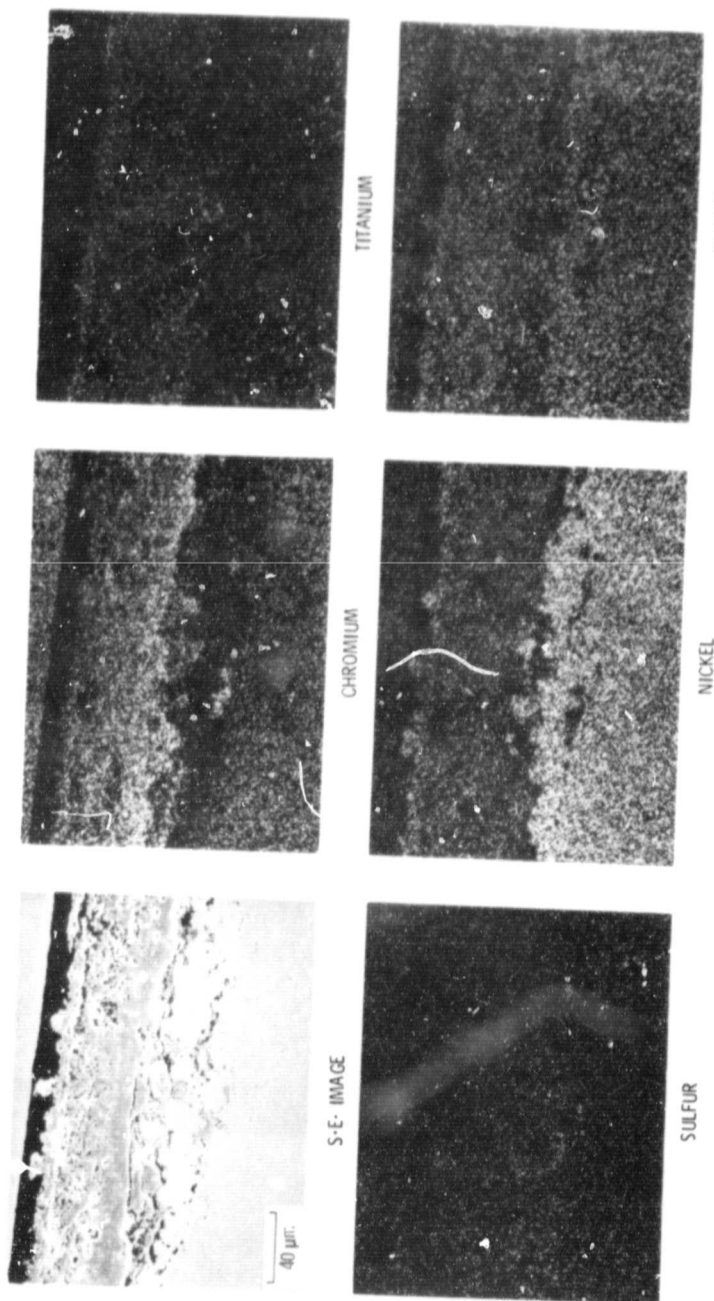


Figure 7. - S. E. image and X-ray maps for U-700 coated with 4.36 mg/cm<sup>2</sup> Na<sub>2</sub>SO<sub>4</sub> and oxidized for 20 hours at 950°C.

ORIGINAL PAGE IS  
OF POOR QUALITY.

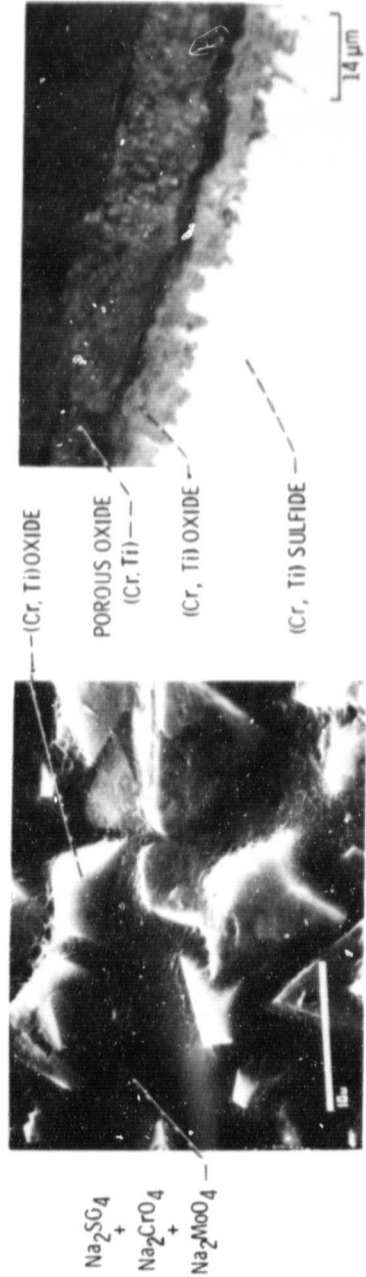
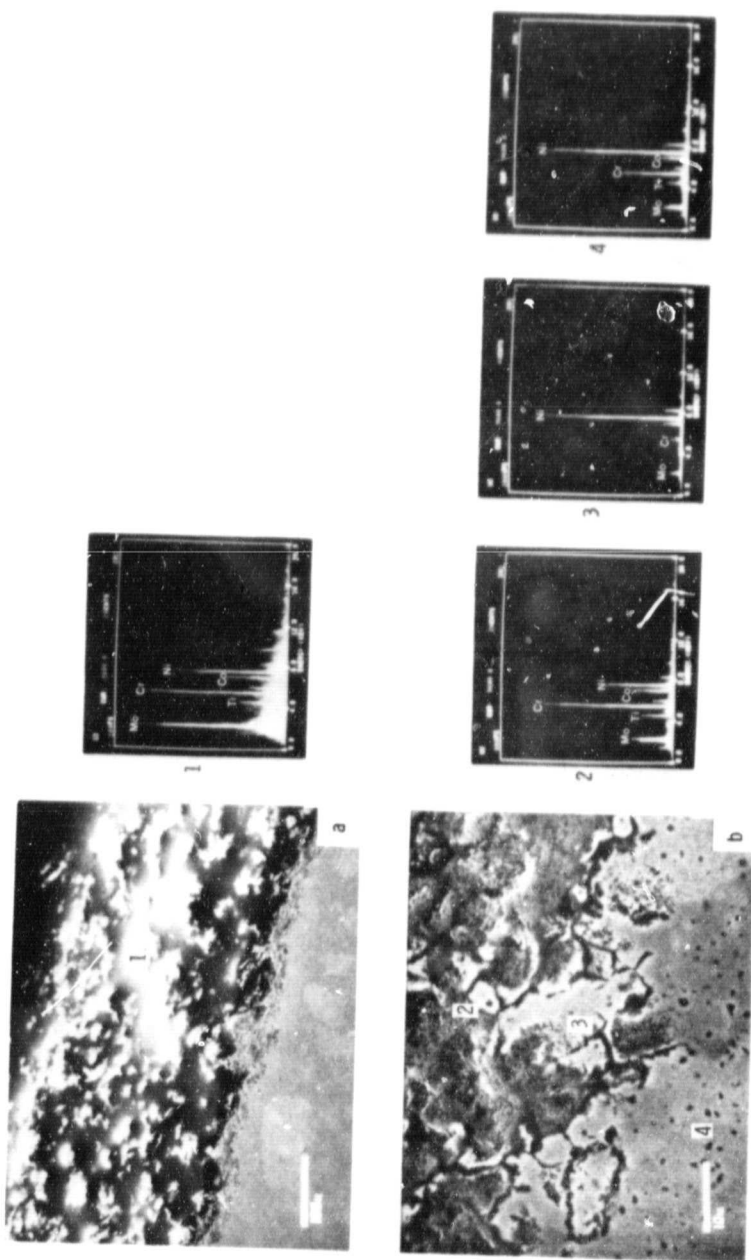


Figure 8. - Top surface and cross-section of U-700 coated with 1.16 mg/cm<sup>2</sup> Na<sub>2</sub>SO<sub>4</sub> and oxidized for 15 hours at 950°C.

ORIGINAL PAGE IS  
OF POOR QUALITY



(a) OVERALL VIEW

(b) SCALE-METAL INTERFACE

Figure 9. - Cross-section of U-700 coated with 0.3 mg/cm<sup>2</sup> Na<sub>2</sub>SO<sub>4</sub> and oxidized for 7 hours at 950°C.

ORIGINAL PAGE IS  
OF POOR QUALITY

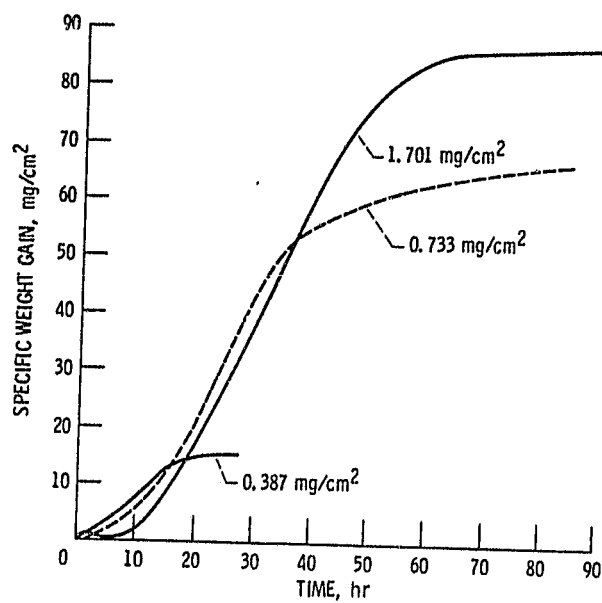


Figure 10. - Kinetics of corrosion of U-700 at 950° C as a function of the amount of Na<sub>2</sub>MoO<sub>4</sub>.

ORIGINAL PAGE IS  
OF POOR QUALITY

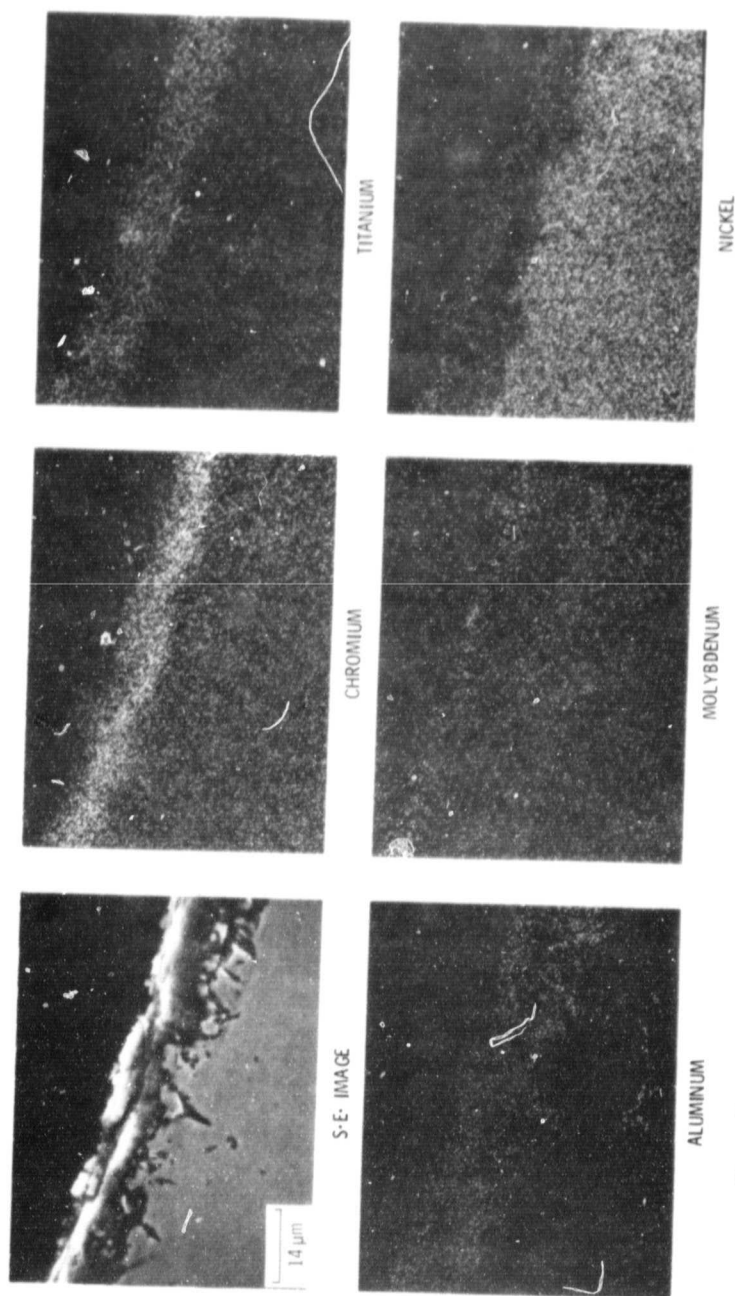


Figure 11. - S. E. image and X-ray maps of U-700 coated with  $0.3 \text{ mg/cm}^2 \text{ Na}_2\text{SO}_4$  and oxidized for 35 hours at  $950^\circ \text{C}$ .